YTUP

Journal of Thermal Engineering

https://jten.yildiz.edu.tr/

https://doi.org/10.47481/jten.0039

RESEARCH ARTICLE

Effect of symmetric and asymmetric non-uniform magnetic field on hydrodynamically developed and thermally developing ferrofluid flow through a circular cross-sectional mini channel

Danvendra Singh[1,2,*], Om Prakash[3]

[1]Department of Mechanical Engineering, National Institute of Technology, Patna, 800005, India
[2]Department of Mechanical Engineering, Gaya College of Engineering, Gaya, 823003, India
[3]Department of Mechanical Engineering, National Institute of Technology, Patna, 800005, India

Abstract

This study examines the heat-transfer characteristics of the hydrodynamically established, thermally developing flow of ferrofluid (Fe_3O_4 + water) in a 2-mm-diameter circular channel under the influence of both symmetric and asymmetric non-uniform magnetic fields. The Langevin function is employed to induce magnetization in ferrofluid nanoparticles when they are subjected to a magnetic field. All instances are analyzed under the parameters of a constant heat flux (q" =1000 W/m^2) condition and within a low Reynolds number spectrum (20-100). Therefore, heat transfer augmentation is facilitated by the application of a magnetic field, which induces a recirculation zone within the flow domain. Systematic analysis revealed that an asymmetric non-uniform magnetic field significantly outperforms the symmetric configuration in both the local and space-averaged Nusselt numbers, especially at a lower Reynolds number (Re=20). The specific angular position of the magnet is critical, as it produces the field's asymmetry and the resulting hydrothermal impact. Among the cases studied, the magnet angular orientation at $\theta = 135^{o}$ proved to be optimal, resulting in a substantial 129.8% increase locally and a 23.54% enhancement in the overall heat transfer effect.

Keywords: Nano particles, ferrofluids, heat transfer, magnetic field, recirculation zone

Cite this article as: Singh, D., & Prakash, O. (2026). Effect of symmetric and asymmetric non-uniform magnetic field on hydrodynamically developed and thermally developing ferrofluid flow through a circular cross-sectional mini channel. Journal of Thermal Engineering, 12(4), 1403–1415. https://doi.org/10.47481/jten.0039

1.Introduction

Over the last two decades, numerous studies have shown that nano-engineering and nano-science have considerable potential to drive technological advancement in the new century. The rapid incorporation of micro- and nano-electromechanical systems (MEMS and NEMS) into modern instrumentation (microfluidic devices, accelerometers, microphones, computers, and smartphone chips) has opened new dimensions in technology. As on one hand, it has provided solutions to miniaturizing the real system, while on the other, it has increased the high-power consumption and elevated operating temperatures [1]. Reduction in size with these systems has posed many challenges in front of technologists and scientists. As device size decreases, conventional heat transfer mechanisms become inefficient, requiring innovative methods to improve system performance and provide targeted cooling and heating of these devices. Because system size is reduced, flow and heat-transfer characteristics are significantly altered and become more restrictive. It does not allow flow at higher Re; therefore, fluid mixing and heat-transfer capabilities are mainly limited to laminar flow. At the same time, the heat transfer capabilities of single-phase laminar flow are limited; therefore, new solutions are required to improve thermal performance. Solutions must be sought at different levels, such as modifying the flow geometry using micro-ribs or turbulators, exploring different rheological fluids with improved thermophysical properties, such as nanofluids and ferrofluids, and employing phase-change processes to utilize latent heat to increase the heat transfer coefficients. Although phase-change systems are more effective, controlling the flow regime is challenging; therefore, many researchers have sought solutions solely within the

*Corresponding Author
E-mail Adress: danvendras.phd19.me@nitp.ac.in

Submitted: 3 November 2025; **Accepted:** 8 February 2026

This paper was recommended for publication in revised form by Editor-in-Chief Ahmet Selim Dalkılıç

Published by Yıldız Technical University, İstanbul, Türkiye
This is an open access article under the CC BY-NC license (http://creativecommons.org/licenses/by-nc/4.0/).

single-phase flow domain. A few years back, ferrofluids [2] (metal oxide nanoparticles dispersed in conventional base fluids like water, ethanol, etc.) with better thermophysical properties attracted attention to serve as efficient heat transfer fluids. By manipulating the position of an external magnet, ferrofluids enable 'targeted cooling,' allowing heat transfer to be focused precisely on specific hot spots. Traditional cooling fluids, however, provide general heat dissipation and lack the precision required for such compact geometries. In contrast, ferrofluids offer a distinct advantage over conventional methods due to their magnetic controllability. So, keep in mind the importance and characteristics of ferrofluid under the impact of varying nanoparticles concentration and magnetic fields, as these factors can significantly affect their performance and stability. Understanding how to optimize ferrofluid behavior, many researchers are exploring experimental techniques and computational models that can predict the response of ferrofluids under different operational conditions.

A two-dimensional (2-D) numerical investigation of ferrofluid flow dynamics was conducted employing both active methodologies (utilizing magnetic fields) and passive approaches (incorporating internal fins and obstructions) to augment heat transfer. This was achieved by computing ferrofluid magnetization as influenced by magnetic susceptibility, which is contingent upon fluid temperature. The examination of the various outcomes indicates that the simultaneous application of both the asymmetric uniform magnetic field and the fins result in a considerably more effective system [3,4]. A 2-D numerical investigation was conducted to analyze ferrofluid behavior within a channel containing symmetric and asymmetric cavities under symmetric uniform and nonuniform magnetic fields. The data demonstrate that an enhancement in the magnetic field intensity corresponds to a decline in the heat transfer rate [5–7]. Natural convection of ferrofluid filled enclosure with different obstacles under the symmetric uniform magnetic field is investigated [8]. Natural convection of ferrofluid in a porous cavity under a symmetric magnetic field reported that heat transfer enhances with Rayleigh number and volume fraction but decreases with increasing Hartmann number [9]. Numerical analysis of natural convection in a cavity containing a wavy conductive cylinder explained that the internal block geometry plays a main role in controlling heat transfer and flow patterns under magnetic fields [10]. A numerical analysis of the combined effect of thermogravitational and magnetic forces within a vertical layer was conducted using the pseudo-spectral Chebyshev method in an asymmetric magnetic field, concluding that flow stability increases with increasing magnetic inclination and that the overall instability pattern shifts toward the heated wall [11]. Numerical studies employing the FVM-MAC scheme for hybrid nanofluids in porous enclosures demonstrated that elevated Rayleigh and Darcy numbers substantially enhance heat transfer, while the application of magnetic fields especially localized ones, efficiently mitigates convection and providing accurate thermal regulation [12,13]. In the scenario involving oscillating magnetic fields, the rectangular waveform frequency function demonstrates superior enhancement in comparison to other conventional waveform functions [14]. The phenomenon of forced convection in ferrofluid flow, characterized by one thermally insulated wall and another subjected to heating in the occurrence of a uniform magnetic field, is investigated, and the role of recirculation is deemed critical for the enhancement of heat transfer efficiency [15–17].

In two-dimensional analysis, explaining the complexities of ferrofluid flow under the influence of a magnetic field presents a significant challenge because one dimension is often neglected, complicating accurate interpretation of the resulting phenomena. Using the finite volume method, three dimensional (3-D) Numerical analysis shows that Kelvin body forces from a periodic non uniform magnetic field produce flow fluctuations, resulting in a maximum 8 % heat transfer enhancement with only a 0.5% rise in friction [18]. Numerical studies in a closed channel with constant heat flux under non uniform magnetic field indicated that magnetic fields accelerate heat transfer by altering flow patterns, with the most significant enhancement observed at lower flow where magnetic forces are not suppressed by inertia [19,20]. Numerical investigations into magnetically induced swirling flows and dipole configurations revealed that non uniform magnetic fields successfully reduce flow resistance while meaningfully enhancing convective heat transfer through boundary layer disruption and fluid mixing [21,22]. Investigations using both laminar and turbulent models in a square cross-sectional channel revealed that uniform magnetic fields generate oscillatory flows, increasing heat transfer by up to 24%, particularly when magnetic field intensity is high and perpendicular to the flow [23,24]. Numerical studies across various applications (including annular ducts, triple-tube heat exchangers, parabolic solar collectors, and permanent magnet machines) demonstrate that uniform transverse magnetic fields induce secondary and swirling flows that significantly enhance heat transfer. Studies confirm the usefulness of ferrofluids with thermal efficiency gains of up to 68% [25–28].

The hydrodynamically and thermally developed flow characteristics of ferrofluid in a metallic tube subjected to a constant heat flux and influenced by a symmetric, uniform magnetic field produced by a permanent magnet beneath the tube have been experimentally examined by numerous researchers. The findings show that the application of a magnetic field significantly improves the Nusselt number [29–32]. Experimental thermal analyses were performed on various types of heat exchangers filled with ferrofluid and subjected to a non-uniform magnetic field. The thermal performance was evaluated under different Reynolds numbers, nanoparticle concentrations, and magnetic field intensities [33–35]. The phenomenon of forced convection heat transfer of ferrofluid situated between two parallel plates under varying conditions in the occurrence of a magnetic field has been rigorously examined through experimental methods. The findings illustrate a significant enhancement in heat transfer attributed to modifications in the thermal boundary layer and in the spatial distribution of magnetic particles [36,37]. The application of a transient non-uniform magnetic field serves to modify the flow characteristics of ferrofluid within a channel. The greatest augmentation of the Nusselt number is observed in comparison to a constant

magnetic field [38,39]. An experimental and computational fluid dynamics (CFD) analysis was conducted to assess laminar forced convective heat transfer and friction factors of Fe_3O_4 nanofluid in a plain cylindrical cross-section duct with twisted tape inserts under varying electromagnetic flux densities. Results indicate that the implementation of twisted tapes with Fe_3O_4 nanofluid under magnetic influence significantly improves heat transfer performance compared to distilled water across all Reynolds numbers [40].

In experimental research, the thermocouple is predominantly used to measure the channel wall temperature. However, the temperature of the channel wall along its periphery is likely to exhibit variation due to ferrofluid circulation, which generates a temperature gradient within the flow. Consequently, to attain a comprehensive understanding of the underlying phenomena, a three-dimensional computational analysis is deemed essential. In the studies, a uniform, symmetric magnetic field is mainly employed to generate the Kelvin body force acting upon the ferrofluid particles, but research on asymmetric, non-uniform magnetic fields requires greater attention to open new directions for findings. Targeted hotspot cooling in electronics remains a challenge that traditional methods often fail to solve. While the use of ferrofluids under magnetic fields is a known solution, most research has been limited to high Reynolds numbers and symmetric, uniform magnetic field arrangements. This creates a clear research gap: the impact of asymmetric non-uniform magnetic fields at low Reynolds numbers (Re<100) is largely unexplored. Our study is motivated by the understanding that heat transfer can be significantly enhanced not only by applying a magnetic field, but also by optimizing the angular orientation of the magnet. Therefore, our main objective is to systematically investigate and compare symmetric and asymmetric non-uniform magnetic-field configurations to maximize the thermal effect both locally and throughout the system in low-velocity flows that are hydrodynamically developed and thermally developing.

2. Methodology

2.1. Computational geometry

A schematic representation of fluid flow, thermal conditions, and magnetic configuration in the microchannel is shown in Figure 1. A cylindrical microchannel with a constant diameter of 2 mm throughout the 20 mm length L is used for ferrofluid flow under hydrodynamically developed and thermally developing conditions. To produce the magnetic field in and around the tube, permanent magnets with a diameter of 1 mm and a length of 2 mm are used. Magnets are positioned above the tube along the x-axis by maintaining a gap to produce symmetric and asymmetric non-uniform magnetic fields. For heat transfer analysis, four simple arrangements are used, as shown in Table 1.

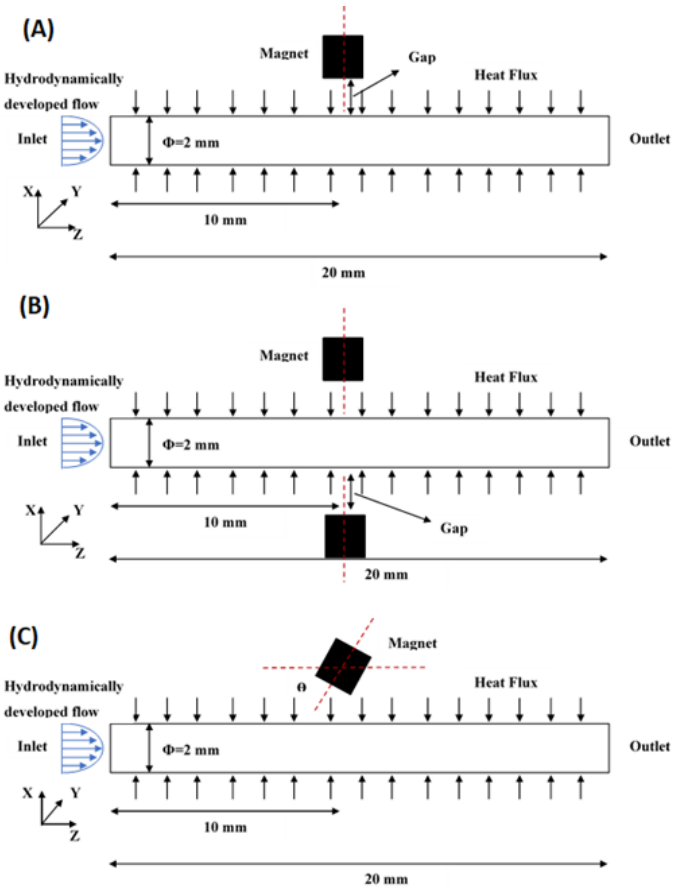

Figure 1. Schematic diagram of microchannel with different magnetic configuration **(A)** case 2 **(B)** case 3 **(C)** case 4

Table 1. Geometry configuration of computational model

Case	Description
Case 1	Without magnetic field (Base case)
Case 2	Symmetric and Non-uniform magnetic field beneath the magnet by a single inline magnet arrangement with 1 mm gap
Case 3	symmetric and non-uniform magnetic field beneath the magnet by a double inline magnet arrangement with 1 gap.
Case 4	Asymmetric and non-uniform magnetic fields changing angular position of magnet (θ=45o, 90o, 135o, 180o,) for 1 mm gap.

2.2. Numerical approach and governing equations

In this study, COMSOL Multiphysics was applied to model the coupled behavior of fluid flow, heat transfer, and magnetic fields. The fluid flow and thermal energy equations are solved using a stationary linear AMG (Algebraic Multigrid) GMRES (Generalized minimal residual) solver with a relative tolerance of 0.001. This solver configuration includes a smoothed-aggregation AMG solver

with SSOR (Symmetric Successive Over-Relaxation) pre-smoother and post-smoother. Furthermore, the magnetic field equations are solved using the conjugate gradient method with a residual tolerance of 0.001. The computational mesh is highly refined, and the total number of degrees of freedom (DOF) used in computational study is 43,100,279.

Ferrofluid is considered a single-phase, electrically non-conducting, homogeneous, Newtonian, and incompressible fluid. These assumptions are physically justified by the specific operating conditions considered, mainly small spherical magnetite particle size (d=10 nm), low volume concentration (Ø=0.02), low Reynolds number and low magnetic field intensity regime. At low magnetic field strengths, the magnetic torque acting on the very small and less concentrated suspended nanoparticles is insufficient to significantly overcome thermal agitation (Brownian motion) [41]. So, the formation of long particle chains or large aggregates which are mainly responsible for inducing non-Newtonian shear-thinning behavior and the magnetoviscous effect is minimal. Under these conditions, the rotational viscosity component arising from the misalignment of magnetic moments remains negligible compared to the hydrodynamic shear viscosity. Therefore, we can reasonably assume constant fluid properties.

Nanomagnetic particles in ferrofluids become magnetized in the presence of an external magnetic field, i.e., one generated by a permanent magnet. This magnetized ferrofluid experiences a magnetic force in the vicinity of a magnetic field, corresponding to the Kelvin body force. This external force disturbed the hydrodynamic and thermal boundary layers of the ferrofluid flow. The flow physics is basically governed by the continuity, momentum, and energy equations as given below [27,38,42]:

Continuity equation:

$$\rho_{ff} \nabla . V = 0 \tag{1}$$

The momentum equation is the consequence of Newton's second law of motion applied to a fluid control volume:

$$\rho_{ff} V . \nabla V = \nabla . [-p + \mu_{ff} (\nabla V + \nabla V^{T})] + F_{mag} \tag{2}$$

Energy Equation:

$$V . \nabla T = \left(\frac{k_{ff}}{\rho_{ff} C_{pff}} \right) \nabla^{2} T \tag{3}$$

2.3. Magnetic field and kelvin body force

The last term on the right-hand side of the equation (2) represents the Kelvin body force. This Kelvin body force is calculated by solving the following equations:

By considering non conduction of ferrofluid and current free of surrounding air, the Maxwell-Ampere's law for magnetic field (H) and flux density (B) by Gauss law is expressed as [41]:

$$\nabla \times H = 0 \tag{4}$$

$$\nabla \cdot B = 0 \tag{5}$$

Magnetic remanent flux density (B_r) is used in the permanent magnet for generating magnetic field (H). Within the magnet, it is expressed as [38]:

$$\nabla . (\mu_0 \mu_{rec} H + B_r) = 0 \tag{6}$$

Here, μ_0 and μ_{rec} represent, respectively, the magnetic permeability of free space and the recoil permeability of the magnet. The magnetic field generated by the permanent magnet magnetizes the ferrofluid. To get the relation between the magnetic field and the magnetization of ferrofluid, Langevin's classical theory is adopted [42].

$$\frac{M}{Ø M_d} = \left(\coth\alpha - \frac{1}{\alpha} \right) = L(\alpha) \tag{7}$$

$$\alpha = \frac{\pi \mu_0 M_d d^3 H}{6 k_b T} \tag{8}$$

Here, α represents the interaction of magnetic and thermal energies of ferroparticles. For large values of α, L(α) moves towards unity. It means that the magnetization of ferrofluid reaches a saturated condition. It can be clearly understood in Figure 2 between the magnetization of ferrofluid and the applied magnetic field.

Magnetic flux density and magnetic field for the ferrofluid are expressed as [38].

$$\nabla . (\mu_0 (H + M)) = 0 \tag{9}$$

With the help of the above equations (7) and (8), equation (9) is modified as:

$$\nabla . \left(\mu_0 \left(H + Ø M_d \left(\coth \left(\frac{\pi \mu_0 M_d d^3 H}{6 k_b T} \right) - \frac{6 k_b T}{\pi \mu_0 M_d d^3 H} \right) \right) \right) = 0 \tag{10}$$

Here Ø represents the volume concentration of the nanoparticles, d is the diameter of Al2O3 nanoparticles and Md (4.46×10^5 A/m) is the domain magnetization of magnetite nanoparticles. Table 2 summarizes the parameters used to simulate the magnetic field of the NdFeB permanent magnet.

Table 2. Parameter used for magnetic field simulation

Parameter used for the magnetic field simulation	
Remanent Magnetic flux density (B_r)	1 T
Recoil permeability of the permanent magnet (NdFeB)	1.05
Magnetic permeability of free space (μ_0)	$4\pi \times 10^{-7}$
Relative permeability of air	1

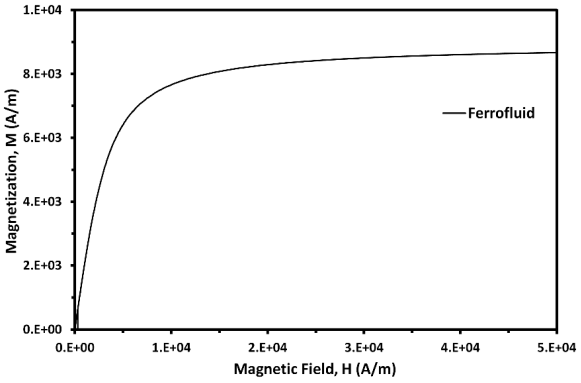

Figure 2. Magnetization of ferrofluid

Magnetic force or Kelvin body force on the magnetized ferrofluid is defined as [19]:

$$F_{mag} = \mu_0 (M.\nabla)H \tag{11}$$

Simplifying the Kelvin body force with help of the above equation (7), we get:

$$F_{mag} = \mu_0 \, \emptyset \, M_d L(\alpha) \nabla H \tag{12}$$

The governing equations mentioned above have been solved using the finite element method. The discretization scheme is based on a second-order formulation for the velocity field and a linear formulation for the pressure and temperature fields. The Navier-Stokes equations are solved to obtain the velocity field of the ferrofluid. The energy transport equation is solved using the previously obtained velocity field to obtain the temperature field. To solve the above-mentioned equations, different models use separate boundary conditions.

For the present simulation study, different boundary conditions were used to solve the above-mentioned equations. To get the magnetic field for the entire domain, the magnetic insulation (n.B=0) boundary condition is considered at the wall boundary. The continuity and momentum equations are solved by assuming a hydrodynamically developed velocity profile, an average inlet velocity, and atmospheric pressure at the channel outlet. The no-slip condition is applied at the channel surface.

$$V_{avg} = \frac{Re \times \mu_{ff}}{\rho_{ff} \times D_h}, \;\; u = 0, \;\; v = 0, \;\; w = 0, \;\; p = 0 \tag{13}$$

To obtain a second-order solution of the energy equation, a thermally developing flow with a uniform fluid temperature of 300 K was maintained at the channel inlet, and diffusive heat conduction at the outlet was set to zero. A constant heat flux is applied to the channel wall.

$$T_{in} = 300 \text{ K}, \;\; n.(-k_{ff} \nabla T) = 0, \;\; q'' = n.(-k_{ff} \nabla T) = 10000 \, \frac{W}{m^2} \tag{14}$$

To understand the heat transfer phenomenon of ferrofluid in the presence of magnet, we use the local Nusselt number and space average Nusselt number from the obtained velocity and temperature solution as per equations (15) and (17).

Local Nusselt Number:

$$Nu_z = \frac{q'' \times D_h}{k_{ff}(T_{wall,z} - T_{ff,z})} \tag{15}$$

Here, $T_{ff,z}$ represents the bulk fluid temperature at a particular section in the fluid flow domain. Average Nusselt Number

$$T_{ff,z} = \frac{\iint V \cdot T dA}{\iint V dA} \tag{16}$$

$$Nu_{avg} = \frac{\int_0^L Nu_z dz}{L} \tag{17}$$

2.4. Material properties

In the present study, a ferrofluid solution (Fe_3O_4+ water) prepared by mixing 2% (v/v) Fe_3O_4 nanoparticles with water was used. The bulk density, specific heat, thermal conductivity, and dynamic viscosity of the ferrofluid are estimated by the commonly quoted and accepted correlation [43,44] given below.

$$\rho_{ff} = \emptyset \, \rho_{np} + (1 - \emptyset)\rho_w \tag{18}$$

$$C_{pff} = \frac{\emptyset \, \rho_{np} C_{p,np} + (1 - \emptyset)\rho_w C_{p,w}}{\rho_{ff}} \tag{19}$$

$$k_{ff} = k_{np}\left[1 + \frac{3\left(\frac{k_{np}}{k_w} - 1\right)\emptyset}{\left(\frac{k_{np}}{k_w} + 2\right) - \left(\frac{k_{np}}{k_w} - 1\right)\emptyset}\right] \tag{20}$$

$$\mu_{ff} = \mu_w (1 + 2.5 \emptyset) \tag{21}$$

The thermophysical properties of the ferrofluid are summarized in Table 3.

Table 3. Materials properties

	Density, ρ (kg/m^3)	Thermal Conductivity k ($W\ m^{-1}\ K^{-1}$)	Specific Heat Cp ($J\ kg^{-1}K^{-1}$)	Viscosity μ (Pa.s)
Fe_3O_4 nano particles	5180	80	670	-
Distilled water	995	0.6	4180	0.0009
Ferrofluid (water + 2 % v/v, Fe_3O_4)	1078.7	0.6359	3842.9	0.000945

2.5. Mesh independency and validation

A fine tetrahedral non-uniform grid has been used in the computational domain, as can be seen from Figure 3 (i). Fine boundary layers have been provided near the walls of the fluid domain to accurately capture the temperature and velocity gradients. To ensure that the results are independent of grid size, a grid independence test was performed. Figure 3 (ii) shows the grid independence test where the variation of the local Nusselt number along the flow direction for various grid sizes is shown. Changing the mesh from 3 to 4 resulted in negligible changes. Hence, we chose mesh 4 to improve the accuracy of the results. Details of the mesh configuration are given in Table 4.

Table 4. Different mesh sizes for fluid flow region and total number of mesh element

Min element size (mm)		No. of element in fluid flow region	Total no. of element
Mesh 1	0.26	136749	200381
Mesh 2	0.22	215117	298148
Mesh 3	0.18	337787	447750
Mesh 4	0.14	656423	818262

Before gaining insight into the flow physics of the ferrofluid, we validated our computational models against established literature to increase confidence in the results. The current problem has two aspects, a heat transfer study and a magnetic field study. Therefore, we have validated both aspects separately. As an initial part of the validation process, the models were first validated with the Shah and London equations [45] of Nusselt number variation along the flow for hydrodynamically developed and thermally developing flow with constant wall heat flux condition. Figure 4 (i) shows that the results obtained in the present work are in very good agreement with the value obtained from the correlations given in equation (22). Shah and London equations for the hydrodynamically developed and thermally developing flow:

$$Nu_{z,H} = \begin{cases} 1.302\,(z^*)^{-1/3} - 1 & \text{for } z^* \le 0.00005 \\ 1.302\,(z^*)^{-1/3} - 0.5 & \text{for } 0.00005 \le z^* \le 0.0015 \\ 4.364 + 8.68\,(1000z^*)^{-0.506}e^{-41z^*} & \text{for } z^* \ge 0.0015 \end{cases} \quad (22)$$

In the second aspect, the magnetic field result is validated with Asfer et al. [46]. Figure 4 (ii) shows the variation in the magnetic flux density along the centerline in the flow direction. Magnetic flux density decreases as we move away from the magnet. The flux density is higher at the magnet's edge. A very good quantitative and qualitative agreement is seen for the obtained result with that of Asfer et al. [46]. After successfully validating both aspects separately, move forward and couple together these aspects, and validate the result with Shah et al. [19]. Figure 4 (iii) shows the comparison of the coupled physics (i.e., hydrothermal and magnetic) in terms of lower wall temperature variation along the flow direction with the earlier published result of Shah et al.[19]. Negligible variation was observed between them. Now with the confidence gained from this certification, we can proceed with our studies.

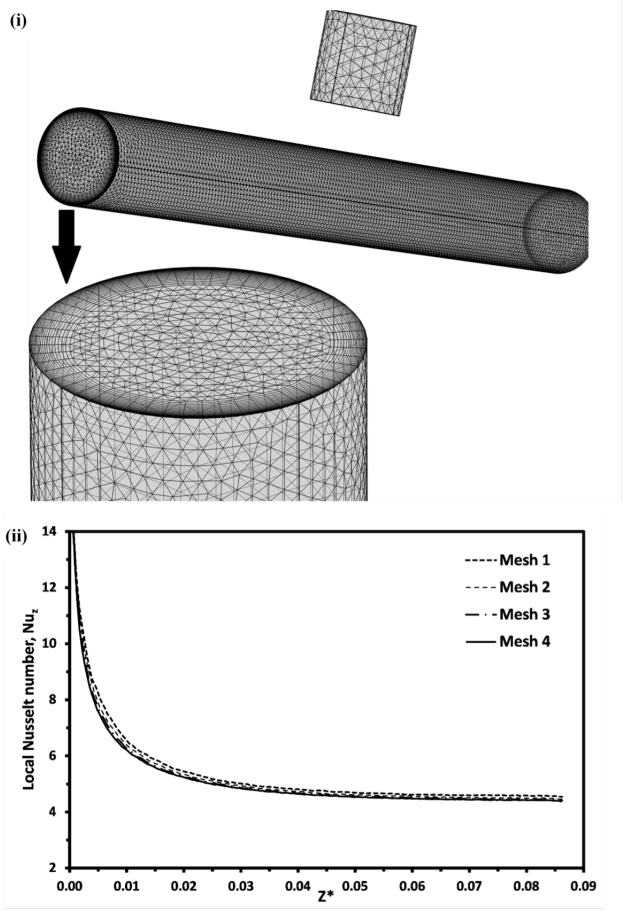

Figure 3. (i) Meshing of computational domain **(ii)** Mesh independency test by using different mesh size

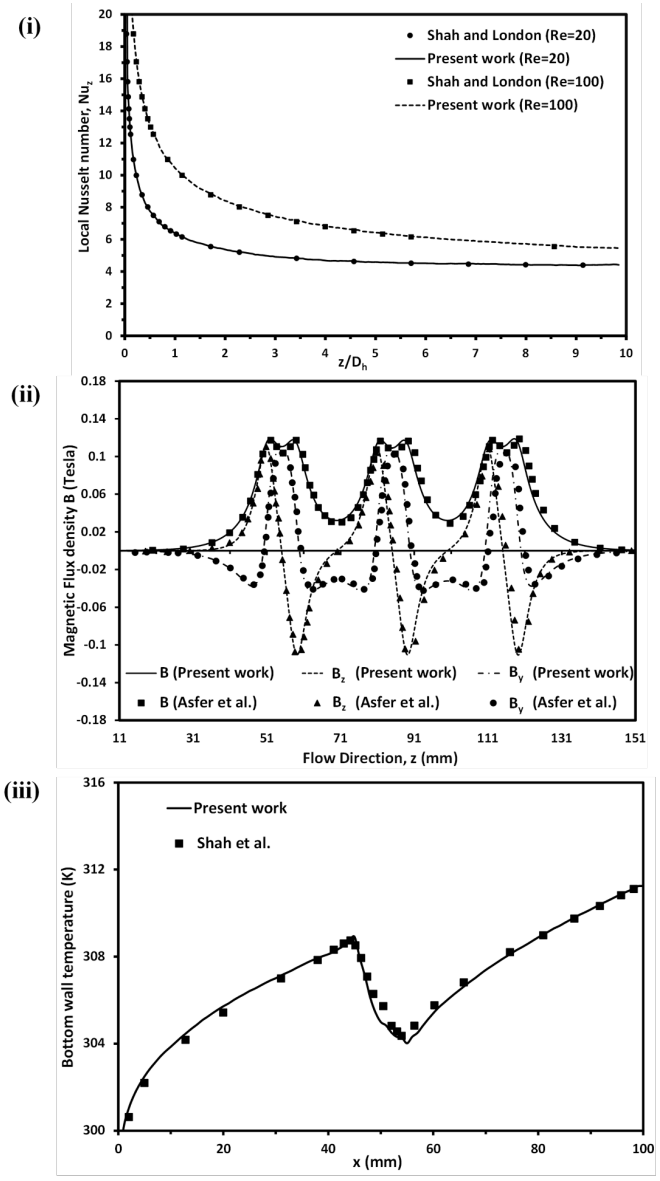

Figure 4. **(i)** Validation graph of present work with Shah and London **(ii)** Magnetic field variation along the centerline of flow channel validation with Asfer et al.[46] **(iii)** Coupled physics (Flow + Magnet) validation with shah et al. [19]

3.Result and discussion

3.1. Variation of magnetic field

Figure 5 (i) shows how the magnetic flux vectors vary in the study domain. It is clear from the vectors that, in cases 2 and 3, symmetric, non-uniform magnetic flux has been applied in the flow domain on both sides of the magnet, whereas in case 4, an asymmetric, non-uniform magnetic field has been applied.

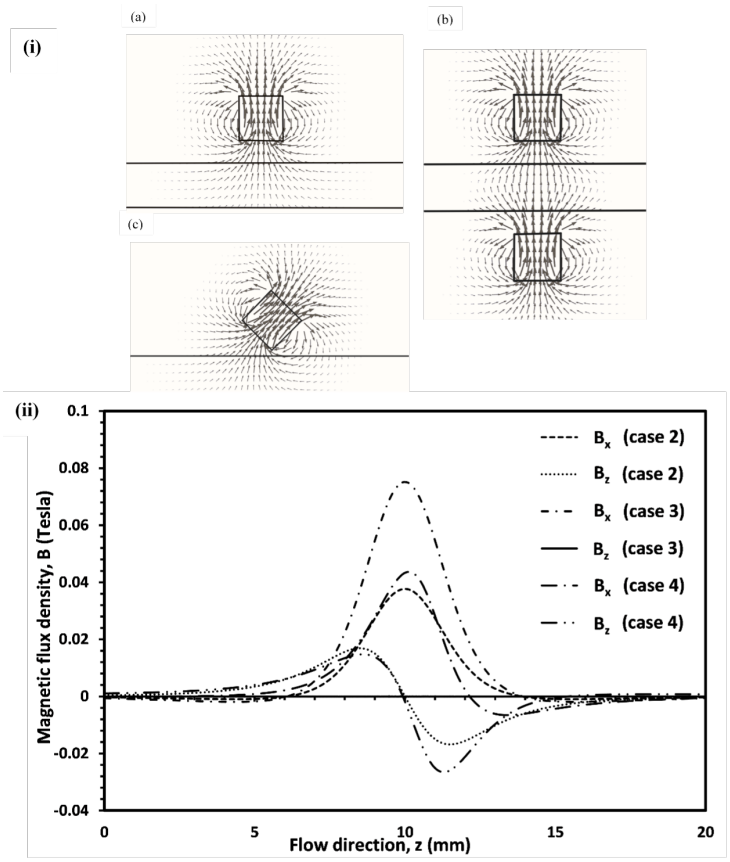

Figure 5. (i) Magnetic flux density vectors (a) case 2 (b) case 3 (c) case 4 (θ=45°) (ii) Magnetic flux density variation along the centre line of the flow channel

Figure 5 (ii) shows how the magnitudes of flux density components vary along the centerline of fluid flow. For cases 2 and 3, away from the magnet, B_x at the centerline is negative because the vector direction changes from upward to downward. On coming closer, the direction of the vector changes upward, causing the maximum value of B_x (the maximum values for case 2 and case 3 are 0.042 Tesla and 0.0765 Tesla, respectively) to be obtained just below the magnet with a positive value. B_x varies similarly on both sides of the magnet along the centerline of the fluid channel. For case 2, the z-component of magnetic flux density, B_z, at the centerline also shows the same pattern on both sides of the magnet but of opposite nature. Its value becomes zero in case 3 because the two magnets are oppositely oriented. In case 4 (θ=45°), because the magnet is angled, the value of B_x on one side decreases on moving away from the magnet and becomes negative, whereas on the opposite side it remains positive. The z component in case 4 (θ=45°) also varies as in case 2, but the magnitude of B_z on both sides of the magnet is different (+ 0.019 Tesla on the left side of the magnet and -0.03 Tesla on the right side of magnet) because of its angular position.

3.2. Effect on hydrothermal characteristics of ferrofluid flow

It is quite clear from Figure 6 (i) that in the left part from the vertical center of the magnet, the horizontal component of the magnetic force (at centerline in the range of F_z=0.42 x 10^5 N/m^3) will be supporting the inertia force. On the other hand, in the right-hand part, it will oppose the inertial force with the same magnitude. Thus, the flow field in the domain results from the resultant of the inertial and magnetic forces. From the velocity vector, it is observable that in upstream locations of the magnet, w' (velocity component in flow direction) velocity increases in the nearby region where magnetic force supports the inertia, while in the downstream locations, a larger magnitude of 'w' is obtained away from the magnet. Fluid on both sides of the magnet feels attraction toward it with a 1.7 x 10^5 N/m^3 maximum magnitude. Due to this attractive force, the velocity vector of the fluid on the left side of the magnet changes direction toward the magnet and increases in magnitude (maximum velocity w = 0.061 m/s). This velocity distribution, the result of the interaction between inertia and magnetic forces, causes disturbances in the boundary layer. This magnet creates a counterclockwise recirculation region, 4.8 mm long and 0.52 mm wide, whose tail end is oriented opposite to the flow direction. Since the velocity vector is changing direction towards the magnet with increasing magnitude, the tail part of this recirculation region in the left part of the magnet acts as a hot region, as the conduction process from wall to fluid is continuous but the advection process is restricted. Consequently, the wall temperature in the tail of the recirculation region increases; as the flow moves downstream, convection intensifies and the wall temperature subsequently decreases. This phenomenon is clearly observed in all cases except case 1 in Figure 6 (ii). This phenomenon is mostly pronounced in case 3. Because the two magnets are face-to-face, the magnetic force only pulls the ferrofluid towards itself, in the direction perpendicular to the magnets' faces within the magnetic field zone. Due to this, recirculation regions (5 mm long and 0.43 mm wide) form near the channel wall, and the advection process becomes very slow. Therefore, the temperature of the wall increases. However, due to the formation of this narrow region beneath the magnet, the velocity of the convective flow increases. Due to this increased velocity, convection intensifies and the wall temperature begins to decrease. In case 4 (θ=135°), the asymmetric magnetic field also causes the magnetic force to appear uneven. Deep recirculation zones (6 mm long and 1.5 mm wide on the left, and 3.5 mm long and 1 mm wide on the right) are formed on both sides of the magnet, thereby disturbing both the thermal and hydrodynamic boundary layers.

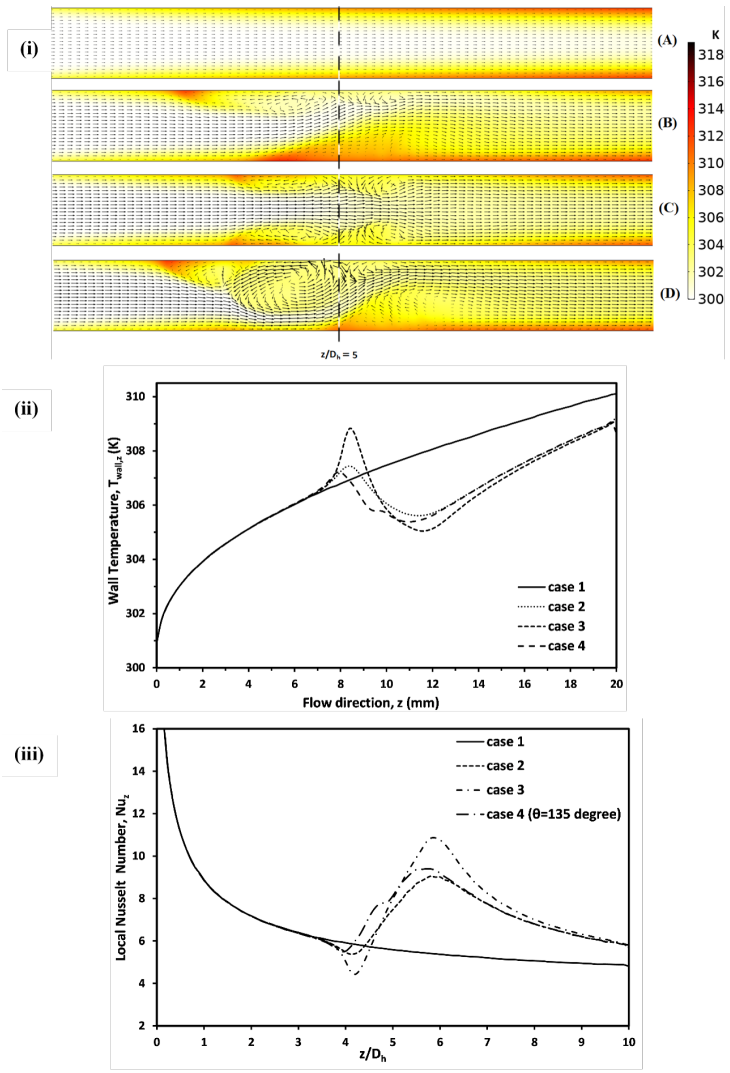

Figure 6. For Re=60 **(i)** Variation of velocity vector and temperature colour contour on zx plane (A) case1 (B) Case 2 (C) Case 3 (D) Case 4 (θ=135^O) **(ii)** Variation of wall temperature **(iii)** Variation of Local Nusselt Number along the direction of flow

3.3. Effect on Nusselt number

The augmentation of the convective heat transfer of ferrofluid under the presence of an external magnetic field mainly depends on the ratio of magnetic to inertial forces acting on the ferrofluid, and on the formation of a recirculation zone. Magnetic force arises from the magnetic field gradient, and the inertial force varies with the flow velocity of the ferrofluid. Figure 6 (iii) shows the fluctuation of the local Nusselt number with respect to the dimensional axial distance (z/D_h) for all examined cases (1 to 4) at Re=60. The graphical representations for all cases show that away from the magnet the Nusselt number decreases to a limiting value owing to the formation of the hot recirculation region; thereafter, when advection becomes

dominant, the Nusselt number increases, reaches a peak, and then declines. In case 4, the progression of the Nusselt number is found to be higher than the increase observed in case 2 for nearly the same magnetic field intensity. This phenomenon can be attributed to the formation of deep recirculation regions, which arise from the asymmetric magnetic field and significantly affect the thermal and fluid dynamics within the system. Case 3, under the influence of a symmetric non-uniform magnetic field, showed a comparatively greater increase in the local Nusselt number (Nu_z=10.86) than the other cases subjected to magnetic fields. This leads to the formation of stagnation recirculation zones in certain regions on the channel wall, which subsequently hinder the efficient transfer of thermal energy and significantly affect the complex interplay of thermal and fluid dynamics within the system. Comparative analysis of the local Nusselt-number increments across cases, relative to case 1, shows that case 4 exhibits the largest increase (73.16%), whereas case 2 shows the smallest increase (67.31%).

3.4. Effect of Reynolds number in symmetric non-uniform magnetic field condition

Extensive numerical investigations covering relevant cases have been carefully conducted at low Reynolds numbers, particularly in the range from 20 to 100, where significant variations in the local Nusselt number have been systematically observed. By carefully analyzing from panels (i) and (ii) of Figure 7, one can observe the complex way the local Nusselt number varies along the specified direction of fluid flow, providing important insights into the thermal performance of the ferrofluid. In a localized context, it has been observed that local enhancement can reach a maximum of 122.68% in case 2 and 177.87% in case 3, representing a significant increase achieved by the application of magnetic fields. Examination of the graphs reveals a significant increase in the local Nusselt number, particularly at low Reynolds numbers. This phenomenon can be attributed to the predominance of magnetic forces under such conditions. Therefore, with increasing Reynolds number, the observed enhancement of the local Nusselt number systematically decreases relative to the initial case.

If one is to analyze extensive changes within the flow field, it becomes imperative to employ equation (17), which provides the mathematical framework for determining the space-averaged Nusselt number and offers a quantitative basis for understanding heat-transfer characteristics in fluid dynamics. Findings from this analytical method indicate that maximum heat transfer predominantly occurs at low Reynolds numbers, demonstrating a significant relationship between heat transfer and Reynolds numbers. Furthermore, as illustrated in Table 5, scenarios characterized by symmetric non-uniform magnetic fields show a clear enhancement in thermal performance, especially at low Reynolds numbers, with Case 2 showing a 21.72% increase and Case 3 showing a 32.01% increase.

Table 5. Space average Nusselt number enhancement by considering base is case1

Re no.	% Increment in Case 2	% Increment in Case 3
20	21.72	32.01
40	16.53	26.90
60	16.04	20.13
80	11.56	13.22
100	07.19	08.95

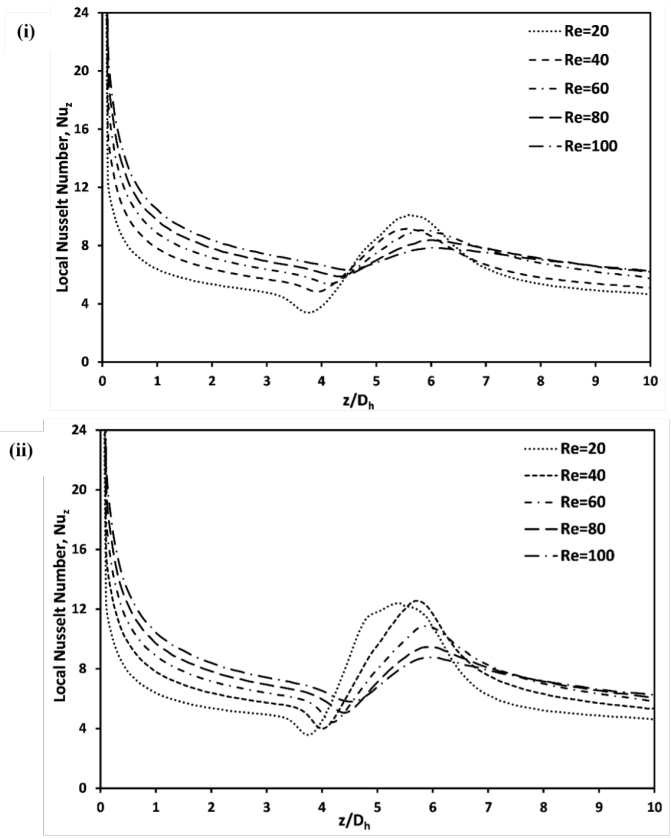

Figure 7. Local Nusselt number change in the flow direction **(i)** case 2 **(ii)** case 3

3.5. Effect of Reynolds number in asymmetric non uniform magnetic field condition

Figure 8 (i) clearly shows that each magnet configuration at Re=20 produces a distinct enhancement of the local Nusselt number, which can be attributed to the differing regions of the magnetic field arising from the magnet orientations. The figure shows how the local Nusselt number changes with the angular position of the magnet relative to the reference axis (i.e., the z-axis). The graph clearly shows a different behavior where the peak of the local Nusselt number shifts toward the left as the angular position of the magnet increases. Furthermore, the magnitude of this peak increases as

the magnet's angular position increases. The maximum local heat transfer is achieved at the θ = 135° magnet position, yielding a peak value of Nu_z = 10.44. This corresponds to a substantial 129.8% local enhancement compared to the base case. By contrast, the peaks for θ = 45° and θ = 90° occur at 10.11 and 10.17, respectively, whereas the θ = 0° and θ = 180° configurations yield a lower peak at 8.68. These results demonstrate that the magnet's position significantly influences heat transfer performance. This variation occurs because the changing position creates an asymmetric, non-uniform magnetic field, exerting distinct magnetic forces that accelerate or decelerate the ferrofluid flow in specific regions.

Having identified that the θ =135° magnet position yields the maximum increment in heat transfer, we continue to investigate how this enhancement behaves across the selected Reynolds number range (20-100). Figure 8 (ii) shows that the largest enhancement occurs at lower Reynolds numbers; as flow velocity increases, the peak local Nusselt number declines. Specifically, we observed a maximum enhancement of 129.8% at Re = 20. This value gradually diminishes to 85.68% at Re = 40, 74.07% at Re = 60, and 54.62% at Re = 80. Finally, at the highest tested velocity of Re = 100, the enhancement reduces to 38.68%.

Figure 8 (iii) depicts the variation of the space-averaged Nusselt number for case 4 across the given Reynolds number range and for all angular positions of the magnet. A remarkably similar enhancement trend was consistently observed across all angular positions assessed in this study. A thorough analysis of the graphical representation indicates that the peak enhancement occurs at the angular position θ = 135°. Notably, an impressive enhancement of 23.54 % is recorded at a Reynolds number of 20, occurring at the magnet's angular position of θ=135°. For the asymmetric nonuniform magnetic field case, a generalized empirical correlation is derived from reported data for the spatially averaged Nusselt number as a function of Reynolds number and magnet inclination angle θ (in degrees). The proposed relation, valid for 20 ≤ Re ≤ 100 and 45 ≤ θ ≤ 180, is expressed as:

$$Nu_{avg} = 4.06 \times Re^{0.17}\left[1 - (3.70 \times 10^{-3})\theta + (3.71 \times 10^{-5})\theta^2 - (1.10 \times 10^{-7})\theta^3\right] \quad (23)$$

This correlation demonstrates excellent agreement with the numerical data, with a mean absolute percentage error of approximately 1.1%, effectively capturing the optimal thermal performance observed near θ =135°.

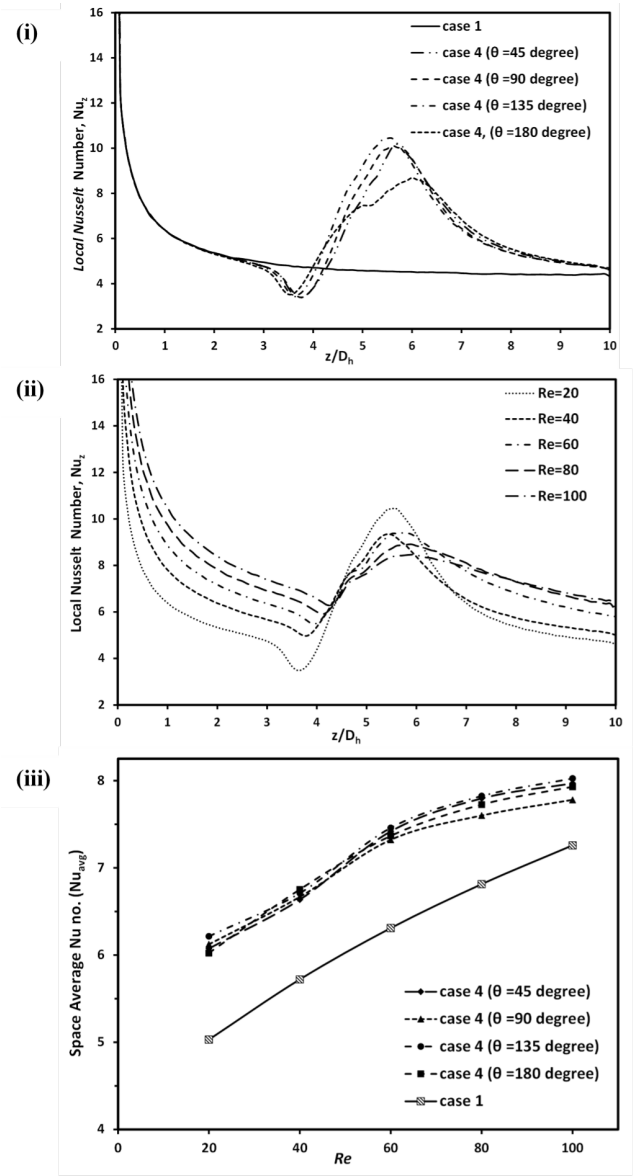

Figure 8. (i) Variation of Local Nusselt Number along the flow direction for case 4 (Re=20) (ii) Variation of Local Nusselt number along the direction of flow, case 4 (θ =135°) (iii) Space average Nusselt Number variation for case 4

4. Conclusion

In this work, a systematic numerical investigation was conducted to analyze the convective heat transfer performance of ferrofluids subjected to symmetric and asymmetric non-uniform magnetic fields. The primary novelty of this study is the exploration of the angular orientation of a magnet as a passive control mechanism for thermal enhancement, specifically within the low Reynolds number range (20-100). The results clearly demonstrate that the enhancement of heat transfer is governed by the interplay between magnetic and inertial forces and the resulting formation of recirculation zones. These findings can be applied in the electronics industry for local-

ized cooling of devices, such as chips and semiconductor components, to improve their efficiency. The principal conclusions drawn from these scenarios are articulated as follows:

- Heat transfer is substantially improved in the presence of a magnetic field because of interactions between magnetic and inertial forces.
- In all cases (except for case 1), the enhancement of heat transfer occurs primarily through the development of recirculation fields exhibiting both clockwise and counterclockwise characteristics, which is facilitated by the interaction between acceleration and deceleration of the ferrofluid in the vicinity of the magnet.
- In Cases 2 and 3, the largest increase in the Nusselt number is recorded at low Reynolds number (Re=20). However, as the Reynolds number increases, the rate of augmentation begins to decline. A localized augmentation in the Nusselt number of 122.68 % and 177.87 %, respectively, is noted in these instances, whereas an overall increase of 21.72 % is documented in Case 2 and of 32.01% in Case 3.
- The magnet's angular position plays a critical role in thermal performance because it generates asymmetric, non-uniform magnetic fields. Magnet position at $\theta=135^{o}$ identified as the optimal position, showing the maximum local Nusselt number enhancement of 129.8% and a space-average enhancement of 23.54% compared to the base case.
- An inverse relationship is observed between the flow velocity and the effectiveness of the magnetic field. The heat transfer augmentation is most pronounced in the low-Reynolds-number regime where magnetic forces dominate inertial forces. Specifically, at the optimal angular position ($\theta=135^{o}$), the local enhancement peaks low Reynolds number but progressively diminishes as inertial forces increase.

The current 3D numerical investigation is restricted to laminar flow under steady-state magnetic fields, in which increasing inertia is observed to suppress thermal enhancement, thereby leaving the impact in turbulent regimes unexplored. Future research should therefore extend this analysis to high Reynolds numbers and examine time-varying or oscillating magnetic fields, which may reduce stagnation zones and optimize performance in dynamic flow environments.

Nomenclature

A	Cross sectional area of channel (m^2)
B_r	Remnant Magnetic Flux density (Tesla)
C_p	Specific Heat of substance ($J\ kg^{-1}\ K^{-1}$)
D_h	Hydraulic diameter of channel (m)
d	Diameter of nanoparticles (m)
F_{mag}	Kelvin body force on Ferrofluid ($N\ m^{-3}$)
k	Thermal conductivity of substance ($W\ m^{-1}\ K^{-1}$)
k_b	Boltzmann's constant (1.38×10^{-23} ($N\ m\ K^{-1}$))
L(α)	Langevin function
M	Magnetization ($A\ m^{-1}$)
M_d	Domain magnetization of nanoparticle ($A\ m^{-1}$)
p	Flow Pressure (Pa)
T	Temperature (K)
u	Velocity component in x direction ($m\ s^{-1}$)
v	Velocity component in y direction ($m\ s^{-1}$)
V	Velocity profile of substance ($m\ s^{-1}$)
w	Velocity component in z direction ($m\ s^{-1}$)
x, y & z	Cartesian coordinates system (m)
Z*	Non dimensional parameter ($z/ (Re\ Pr\ D_h)$)

Greek Symbols

μ	Dynamic Viscosity (Pa s)
ρ	Density ($kg\ m^{-3}$)
θ	Angular position of magnet (in degree)
ϕ	Mini channel diameter (m)
μ_0	Permeability of free space $4\pi \times 10^{-7}$ ($N\ A^{-2}$)
Ø	Volume fraction of magnetic nanoparticles

Subscripts

avg	Average
ff	ferrofluid
mag	magnetic
np	nanoparticles
w	water
in	Inlet

References

[1] Bahiraei M, Heshmatian S. Electronics cooling with nanofluids: A critical review. Energy Convers Manag 2018;172:438–56. https://doi.org/10.1016/j.enconman.2018.07.047.

[2] Choi SUS, Eastman JA, Eastman JA Enhancing thermal conductivity of fluids with nanoparticles. vol. 1. 1935.

[3] Jalali S, Barati E, Kalat MF. Numerical investigation of synergistic effects of magnetic fields and bluff bodies on heat transfer enhancement and pressure drop reduction in microchannels. Results in Engineering 2024;24. https://doi.org/10.1016/j.rineng.2024.102894.

[4] Boutas L, Marzougui M, Zinoubi J, Gannouni S. Impact of Magnetic Fields and Fins on Entropy Generation, Thermal, and Hydrodynamic Performance in the Ferrofluids Flow within a Mini Channel. Journal of Applied Fluid Mechanics 2024;17:658–71. https://doi.org/10.47176/jafm.17.3.2134.

[5] Cunha LHP, Siqueira IR, Campos AAR, Rosa AP, Oliveira TF. A numerical study on heat transfer of a ferrofluid flow in a square cavity under simultaneous gravitational and magnetic convection. Theor Comput Fluid Dyn 2020;34:119–32. https://doi.org/10.1007/s00162-020-00515-1.

[6] Qureshi MA, Hussain S, Sadiq MA. Numerical simulations of MHD mixed convection of hybrid nanofluid flow in a horizontal channel with cavity: Impact on heat transfer and hydrodynamic forces. Case Studies in Thermal Engineering 2021; 27. https://doi.org/10.1016/j.csite.2021.101321.

[7] Hussain S, Öztop HF, Qureshi MA, Abu-Hamdeh N. Magnetohydrodynamic flow and heat transfer of ferrofluid in a channel with non-symmetric cavities. J Therm Anal Calorim 2020;140:811–23. https://doi.org/10.1007/s10973-019-08943-w.

[8] Lee M, Kim YJ. Effect of non-uniform magnetic fields on the characteristics of ferrofluid flow in a square enclosure. J Magn Magn Mater 2020;506. https://doi.org/10.1016/j.jmmm.2020.166697.

[9] Pekmen Geridönmez B. Numerical simulation of natural convection in a porous cavity filled with ferrofluid in presence of magnetic source. vol. 4. Yildiz Technical University Press; 2018.

[10] Tayebi T, Chamkha AJ. Magnetohydrodynamic Natural Convection Heat Transfer of Hybrid Nanofluid in a Square Enclosure in the Presence of a Wavy Circular Conductive Cylinder. J Therm Sci Eng Appl 2020;12. https://doi.org/10.1115/1.4044857.

[11] Rahman MH. Investigation of thermomagnetic gravitational convection and energy distribution in a vertical layer of ferrofluid. Journal of Thermal Engineering 2024;10:936–53. https://doi.org/10.14744/thermal.0000850.

[12] Venkata Lakshmi C, Sri KS, Venkatadri K, Bég OA. Simulation of partial magnetic field effects on Cu-TiO 2 -water hybrid nanofluid natural convection flow in a Darcy–Brinkman–Forchheimer porous media enclosure with a MAC-FVM combined scheme. Int J Comput Mater Sci Eng 2025. https://doi.org/10.1142/S2047684125500228.

[13] Venkata Lakshmi C, Swetha Sri K, Venkatadri K. Computational analysis of magnetized heat transfer in a non-Darcy porous enclosure using ternary hybrid nanofluid and finite volume MAC method. Int J Mod Phys B 2025;39. https://doi.org/10.1142/S0217979225502170.

[14] Salehpour A, Ashjaee M. Effect of different frequency functions on ferrofluid FHD flow. J Magn Magn Mater 2019;480:112–31. https://doi.org/10.1016/j.jmmm.2019.02.045.

[15] Mehrez Z, Cafsi A El. Heat exchange enhancement of ferrofluid flow into rectangular channel in the presence of a magnetic field. Appl Math Comput 2021;391. https://doi.org/10.1016/j.amc.2020.125634.

[16] Shah RK, Khandekar S. Exploring ferrofluids for heat transfer augmentation. J Magn Magn Mater 2019;475:389–400. https://doi.org/10.1016/j.jmmm.2018.11.034.

[17] Nessab W, Kahalerras H, Fersadou B, Hammoudi D. Numerical investigation of ferrofluid jet flow and convective heat transfer under the influence of magnetic sources. Appl Therm Eng 2019;150:271–84. https://doi.org/10.1016/j.applthermaleng.2018.12.164.

[18] Dahmani A, Muñoz-Cámara J, Solano JP, Laouedj S. Thermal-hydraulic analysis of ferrofluid laminar flow in tube under non-uniform magnetic field created by a periodic current-carrying wire. Frontiers in Heat and Mass Transfer 2022;18. https://doi.org/10.5098/hmt.18.42.

[19] Shah RK, Drave JK, Khandekar S. Thermal Transport in Laminar Convective Flow of Ferrofluids in the Presence of External Magnetic Field. J Heat Transfer 2021;143. https://doi.org/10.1115/1.4050411.

[20] Lazim AA, Daneh-Dezfuli A, Habeeb LJ. Numerical Analysis of Heat Transfer Enhancement Using Nanofluid Under Variable Magnetic Fields. Power Engineering and Engineering Thermophysics 2024;3:1–11. https://doi.org/10.56578/peet030101.

[21] Dalvi S, van der Meer TH, Shahi M. Hydro - thermal interactions of a ferrofluid in a non - uniform magnetic field. Heat and Mass Transfer/Waerme- Und Stoffuebertragung 2022. https://doi.org/10.1007/s00231-022-03278-z.

[22] Bezaatpour M, Rostamzadeh H. Heat transfer enhancement of a fin-and-tube compact heat exchanger by employing magnetite ferrofluid flow and an external magnetic field. Appl Therm Eng 2020;164. https://doi.org/10.1016/j.applthermaleng.2019.114462.

[23] Jafari H, Goharkhah M. Application of electromagnets for forced convective heat transfer enhancement of magnetic fluids. International Journal of Thermal Sciences 2020;157. https://doi.org/10.1016/j.ijthermalsci.2020.106495.

[24] Zhang X, Zhang Y. Heat transfer and flow characteristics of Fe3O4-water nanofluids under magnetic excitation. International Journal of Thermal Sciences 2021;163. https://doi.org/10.1016/j.ijthermalsci.2020.106826.

[25] Bakalis PA, Papadopoulos PK, Vafeas P. Heat transfer study of the ferrofluid flow in a vertical annular cylindrical duct under the influence of a transverse magnetic field. Fluids 2021;6. https://doi.org/10.3390/fluids6030120.

[26] Hosseinizadeh SE, Majidi S, Goharkhah M, Jahangiri A. Energy and exergy analysis of ferrofluid flow in a triple tube heat exchanger under the influence of an external magnetic field. Thermal Science and Engineering Progress 2021;25. https://doi.org/10.1016/j.tsep.2021.101019.

[27] Khosravi A, Malekan M, Assad MEH. Numerical analysis of magnetic field effects on the heat transfer enhancement in ferrofluids for a parabolic trough solar collector. Renew Energy 2019;134:54–63. https://doi.org/10.1016/j.renene.2018.11.015.

[28] Zhang W, Li GJ, Qin Y. Comparative Study of Ferrofluid Cooling for Permanent Magnet Machines With Different Winding Structures. IEEE Access 2024;12:18041–50. https://doi.org/10.1109/ACCESS.2024.3359900.

[29] Jiao F, Li Q, Jiao Y, He Y. Heat transfer of ferrofluids with magnetoviscous effects. J Mol Liq 2021;328. https://doi.org/10.1016/j.molliq.2021.115404.

[30] Eslahchi A, Nobakhti MH, Shafii MB, Dibaei Bonab MH. Experimental evaluation of forced convective heat transfer of Fe3O4 ferrofluid in a horizontal u-shaped tube under variable magnetic field effect based on Taguchi approach. Journal of the Brazilian Society of Mechanical Sciences and Engineering 2021;43. https://doi.org/10.1007/s40430-021-02910-z.

[31] Sun B, Guo Y, Yang D, Li H. The effect of constant magnetic field on convective heat transfer of Fe3O4/water magnetic nanofluid in horizontal circular tubes. Appl Therm Eng 2020;171. https://doi.org/10.1016/j.applthermaleng.2020.114920.

[32] Wang J, Li G, Zhu H, Luo J, Sundén B. Experimental investigation on convective heat transfer of ferrofluids inside a pipe under various magnet orientations. Int J Heat Mass Transf 2019;132:407–19. https://doi.org/10.1016/j.ijheatmasstransfer.2018.12.023.

[33] Tekir M. Experimental study on the thermal performance of hybrid nanofluid in a compact plate heat exchanger under the influence of a magnetic field. Case Studies in Thermal Engineering 2025;69. https://doi.org/10.1016/j.csite.2025.106031.

[34] Zheng D, Yang J, Wang J, Kabelac S, Sundén B. Analyses of thermal performance and pressure drop in a plate heat exchanger filled with ferrofluids under a magnetic field. Fuel 2021;293. https://doi.org/10.1016/j.fuel.2021.120432.

[35] Bezaatpour M, Goharkhah M. Convective heat transfer enhancement in a double pipe mini heat exchanger by magnetic field induced swirling flow. Appl Therm Eng 2020;167. https://doi.org/10.1016/j.applthermaleng.2019.114801.

[36] Cheng Y, Li D. Experimental investigation on convection heat transfer characteristics of ferrofluid in a horizontal channel under a non-uniform magnetic field. Appl Therm Eng 2019;163. https://doi.org/10.1016/j.applthermaleng.2019.114306.

[37] Valitabar M, Rahimi M, Azimi N. Experimental investigation on forced convection heat transfer of ferrofluid between two-parallel plates. Heat and Mass Transfer/Waerme- Und Stoffuebertragung 2020;56:53–64. https://doi.org/10.1007/s00231-019-02689-9.

[38] Shyam S, Mehta B, Mondal PK, Wongwises S. Investigation into the thermo-hydrodynamics of ferrofluid flow under the influence of constant and alternating magnetic field by InfraRed Thermography. Int J Heat Mass Transf 2019;135:1233–47. https://doi.org/10.1016/j.ijheatmasstransfer.2019.02.050.

[39] Abadeh A, Sardarabadi M, Abedi M, Pourramezan M, Passandideh-Fard M, Maghrebi MJ. Experimental characterization of magnetic field effects on heat transfer coefficient and pressure drop for a ferrofluid flow in a circular tube. J Mol Liq 2020;299. https://doi.org/10.1016/j.molliq.2019.112206.

[40] Yadav RJ, Mahajani T, Kore SS, Gadhe PM, Kamble DA. Investigation of heat transfer characteristics using Fe3O4 nanofluid along with TT inserts in tube with uniform electromagnetic field. Applied Nanoscience (Switzerland) 2023; 13:763–85. https://doi.org/10.1007/s13204-021-01905-5.

[41] Griffiths DJ. Introduction to electrodynamics. 3rd Edition. New Jersey: Prentice Hall; 1999.

[42] Rosenswei9 RE. MAGNETIC FLUIDS. vol. 19. 1987.

[43] Rea U, McKrell T, Hu L wen, Buongiorno J. Laminar convective heat transfer and viscous pressure loss of alumina-water and zirconia-water nanofluids. Int J Heat Mass Transf 2009;52:2042–8. https://doi.org/10.1016/j.ijheatmasstransfer.2008.10.025.

[44] Kleinstreuer C, Feng Y. Experimental and theoretical studies of nanofluid thermal conductivity enhancement: A review. Nanoscale Res Lett 2011;6. https://doi.org/10.1186/1556-276X-6-229.

[45] Irvine TF, Hartnett JP, Shah RK, London AL. Advances in HEAT TRANSFER Supplement 1 laminar flow forced convection in ducts A Source Book for Compact Heat Exchanger Analytical Data. 1978.

[46] Asfer M, Mehta B, Kumar A, Khandekar S, Panigrahi PK. Effect of magnetic field on laminar convective heat transfer characteristics of ferrofluid flowing through a circular stainless steel tube. Int J Heat Fluid Flow 2016;59:74–86. https://doi.org/10.1016/j.ijheatfluidflow.2016.01.009.